Hybrid Acoustic Model of Electric Vehicles: Force Excitation in Permanent-Magnet Synchronous Machines

Sebastian Rick, Aryanti Kusuma Putri, David Franck, and Kay Hameyer, *Senior Member, IEEE*

***Abstract*—In this paper, an integrated model for acoustic evaluation of electric vehicles is introduced. The paper focuses on the force excitation part of the model. The analysis is performed for permanent magnet synchronous machines. The excitation forces are placed on the stator teeth and calculated for a structure dynamic model of the power train. A model for the acoustic emission is adapted, and finally, the psychoacoustical behavior is characterized at the position of the driver of the e-car. An approach for the design of the rotor pole topology is introduced to ensure a beneficial acoustic behavior under consideration of air gap flux density and related force densities on the stator teeth. The calculation is performed using finite-element analysis simulation, but also analytical design methods are considered. Objective of this comparison is a very short computation time and, therefore, an efficient simulation process. The model is validated by measurements on test benches.**

***Index Terms*—Acoustic design, force density excitation, permanent-magnet synchronous machine (PMSM), psychoacoustics of electrical machines, structure dynamic model.**

I. Introduction

THE purchase behavior for vehicles depends on subjective assessment criteria of the driver. For the design of electric vehicles, the convenience plays a decisive role, for example, referring to noise and vibration phenomena. The modeling of the acoustic behavior in the cabin of electric vehicles is important to ensure a competitive design in comparison to vehicles with combustion engine.

The expectation of the costumer for a comfortable driving experience is influenced by vibrations and noise, which are different to vehicles with combustion engine. For the electrical drive train, a lower absolute sound pressure level is expected, but with more tonal noise at higher frequencies [1]. Also, the noise of other car components, like pumps or auxiliary drives, is not masked by the electrical machine, which comes to a very different hearing experience in the car cabin [2].

In this paper, a model chain for the acoustic evaluation of electric vehicles is introduced. It is based on a paper presented at the 2015 International Electric Machines and Drives Conference [3]. Starting with the driver input in a specific traffic situation and ending with the psychoacoustic experience of this driver [4], the model introduces a wide overview through the acoustic relevant effects in a vehicle. The model is separated into three parts: the force excitation in the electrical machine, the structure dynamic deformation of the participating drive train components [5], and the acoustic emission in the car cabin, reaching the driver‘s ears [6].

The focus in this paper is on the force excitation model, considering the control of the electrical machine, the electromechanical transformation, and the conjunction with the structure dynamic model [7]. Different modeling approaches for the calculation of the force excitation in the machine are presented. A parameter study for different pole topologies is introduced to show the design prospects for electrical machines with this model chain.

The validation of the model is performed with different testing cases, for example, measurements on the components, the drive train, and the entire vehicle are considered. The model is applied to a test carrier, which is the basis for the validation and is described in the next section. A modular design concept allows the exchange of specific components to adopt the presented model to various applications.

II. Concept of Modeling

To introduce the concept of the modeling chain to describe the acoustic behavior of an electric vehicle, the test carrier is presented. The design steps in the modeling process are discussed, and the concepts for validating the acoustic vehicle model are introduced.

A. Test Carrier

In this paper, an electric vehicle of the category compact city car with maximum speed of 130 km/h is used. The battery is placed at the bottom of the car, between front and rear axle. The drive train is situated in the back of the car, beneath the luggage compartment. A typical converter system is used for the control of the machine. In this study, a permanent magnet synchronous machine with interior buried permanent magnets (IPMSM) is considered. The machine has six pole pairs and 36 stator slots.

Manuscript received July 30, 2015; revised January 13, 2016; accepted February 22, 2016. Date of publication March 25, 2016; date of current version July 15, 2016. Paper 2015-EMC-0626. R1, presented at the 2015 IEEE International Electric Machines and Drives Conference, Couer d'Alene, ID, USA, May 10–13, and approved for publication in the IEEE TRANSACTIONS ON INDUSTRY APPLICATIONS by the Electric Machines Committee of the IEEE Industry Applications Society. This work is based upon a collaboration between three institutes of RWTH Aachen University: Institute of Electrical Machines, Institute for Machine Elements and Machine Design, and the Institute of Technical Acoustics. The corresponding research project No. 682 was organized in Forschungsvereinigung Antriebstechnik e. V. in Germany and funded by AiF in the frame work of the program of Industrielle Gemeinschaftsforschung (IGF) by the Federal Ministry for Economic Affairs and Energy (BMWi).

The authors are with the Institute of Electrical Machines, RWTH Aachen University, 52062 Aachen, Germany (e-mail: sebastian.rick@iem.rwth-aachen.de; aryanti.putri@iem.rwth-aachen.de; david.franck@iem.rwth-aachen.de; Kay.Hameyer@iem.rwth-aachen.de).

Color versions of one or more of the figures in this paper are available online at http://ieeexplore.ieee.org.

Digital Object Identifier 10.1109/TIA.2016.2547360

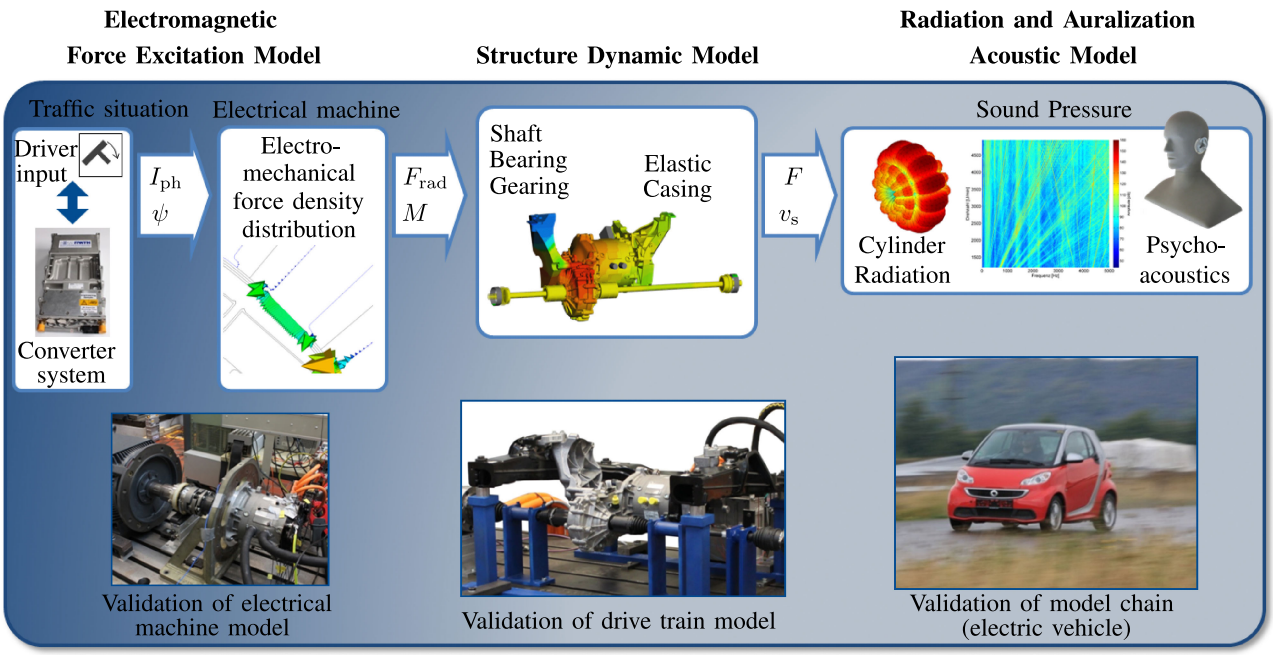

Fig. 1. Structure diagram for model chain of electric vehicle. Model chain is divided into three parts: the force excitation in the electrical machine, the structure dynamic behavior of the drive train, and the acoustic emission correlating to the electric vehicle. Each model is presented, and the interface between them is discussed. The focus is on the electrical machine and thereby on the force excitation part.

The rare earth magnets in the rotor are placed in an I-shape with a center bridge for each pole. The nominal torque of the machine is 130 N·m, and the peak value of the phase current is 300 A. The machine is connected to a gearbox with a transmission ratio of about 10. Different modeling approaches are compared with focus on high resolution and detailed description of the drive train, compatibility to other model parts and fast simulation time. In the first step, the integrated electrical machine of the test carrier is analyzed; in Sections V and VI, the model of the machine is considered for different parameter variations in the rotor geometry. This variation is performed to analyze the acoustical behavior with the chain model of the entire vehicle described in Section II-B. The interface between different model parts is designed and the interaction is considered. The simulations are performed for the entire operating area of the electrical machine to ensure an evaluation in any traffic situation of the vehicle.

B. Modeling Process

The model chain is separated into three main parts: the force excitation model, the structure dynamic model, and the acoustic model (see Fig. 1). A hybrid model concerning simulation parts and measurement parts is developed.

The force excitation model contains the driver‘s input at the accelerator pedal, resulting in an operating point which is controlled in the converter. Electrical operating points are described by the peak value of the phase current I_{ph} and the control angle ψ, which identify a point in the second quadrant of the $i_d i_q$ plane, which is introduced in Section III. Based on the operating point, the simulation of the force excitation in the electrical machine is calculated at the stator teeth. Different approaches are considered for describing the electromechanical force density distribution. The radial force density and the torque are taken as interface parameters between the force excitation model and the structure dynamic model of the drive train. For this reason, the electromagnetic force density distribution on the surface of the stator teeth and the torque distribution of the machine represent the parameters to describe individual machine behavior or design variations of the magnetic circuit.

The structure dynamic model is based on a multibody system, consisting of the subframe of the rear axle of the vehicle, the bearings for the drive train, the electrical machine with cooling system, etc., the gearing with differential, side shaft, and wheel bearing. The force excitation entry of the machine is placed on the tip of the stator teeth and the torque on the slices of the rotor (see Sections III-B2 and V). The corresponding deformation and the vibrations are simulated in a numerical environment. The forces at the bearings of the drive train and the surface velocities of the components are chosen for the interface between the structure dynamic model and the acoustic model.

In the acoustic model, the drive train components are modeled as cylindrical and piston-type elements. The corresponding sound pressure is calculated and basis for the airborne sound in the vehicle. The transfer paths for airborne and structure-borne sound are determined with measurements in the electric vehicle. In the last simulation step, the psychoacoustical interpretation of the sound pressure is performed by psychoacoustic analysis functions (see Section VI).

The entire model chain allows the acoustic evaluation of the vehicle in a closed loop around the driver, concerning his driving style and acoustic impression of the electric vehicle.

C. Validation Process

The validation process of the entire model chain is performed in three steps. In the first step, each component of the drive train

TABLE I
PARAMETERS FOR FORCE EXCITATION MODEL

Symbol	Quantity	Unit	Description
N	36	-	number of stator slots
p	6	-	number of pole pairs
m	3	-	number of phases
γ	0–360	°	mechanical position angle
λ_{rad}	-	-	relative radial stator permeance function
B_{rad}	-	T	radial air gap flux density
F_{rad}	-	N/m^2	radial force density
y	-	m	deformation
v_s	-	m/s	surface velocity
f	-	Hz	frequency
I_{ph}	0–300	A	peak phase current
ψ	0–90	°	control angle
ψ_{opt}	10	°	control angle for nominal operating point
k	120	-	simulation steps of FEA model
θ_{step}	0.5	°	step width of FEA simulation
ν	0, 12, 24 ...	-	spatial order
M	0–130	N·m	torque of electrical machine
n	0–12 000	r/min	speed of electrical machine

is considered independently. Therefore, the electrical machine is measured in a machine test bench, excluding gear and other drive train components. Various parts of the drive train are measured with a modal analysis to investigate their behavior in the structure dynamic model.

In the second step, the drive train is placed in the original setup of the electric vehicle, composed of the components that are analyzed in the first validation step. The resulting test bench gives information of the interaction of different components, for example, electrical machine and gear, and is used as basis for the validation of the drive train.

In the third step, the electric vehicle is measured on a test track. This testing case is also useful for the subjective interpretation of the sound in the car and provides an impression of masking effects and the intensity of the drive trains noise, relating to other driving noise, for example, rolling noise of the wheels.

III. FORCE EXCITATION MODEL

For the force excitation modeling, a simulation of the electrical machine for calculation of electromagnetic fields is developed. Thereby, the force calculation at the stator teeth is provided in a postprocessing step. With the calculated force densities, an interface to the structure dynamic model is defined. General parameters for the force excitation model are presented in Table I.

A. Approaches for Machine Modeling

For the simulation of the electrical machine, three different approaches are distinguished:

1) an analytical approach with design tables;
2) an analytical model based on conformal mapping (CM);
3) a numerical approach based on finite-element analysis (FEA).

In this section, the presented three approaches are discussed, and their advantages and disadvantages are highlighted.

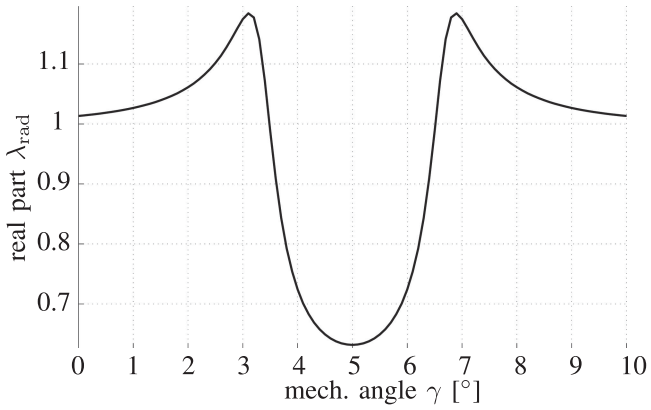

Fig. 2. Stator permeance function for an analytical approach with CM. Real part in radial component. Description for a single slot pitch of the stator (mechanical angle γ for one slot as result of 36 identical stator slots).

1) Analytical Model Based on Design Tables: A general approach for the simulation of force density excitation in electrical machines is presented in [8] with the evaluation in design tables. A corresponding model to this approach is based on machine parameters, in general, the number of stator teeth N, the number of pole pairs p, and the number of phases m. The calculation is performed with appropriate rotating magnetic field theory equations. The model is based on a cylinder approximation of the electrical machine. As result, a design table with frequency and spatial orders for the force excitation is calculated. The composition of the corresponding air gap flux density harmonics, leading to the force density behavior, is reproducible. The application of this force excitation model and the simulation time are short. The results do not include information about the amplitude of different force density harmonics, and the geometry of the electrical machine is not indicated in the simulation process, with the exception of previously presented parameters. A numeric structure dynamic simulation is not adaptable to this model. For this reason, the analytical model, based on design tables, is used in the early modeling process and for validation of further presented approaches.

2) Analytical Model Based on Conformal Mapping: An analytical approach for more detailed simulation of force density excitation in the electrical machine is presented under the topic of CM [9]. In this case, a 2-D cross-sectional model of the machine is constructed, which is based on general machine parameters comparable to Section III-A1 and main physical dimensions such as rotor and stator diameters. The stator teeth geometry is approximated through infinite deep radial flanking slots and radial adapting tooth tip to the air gap. By conformal transformation of this geometry, the magnetic field distribution is describable by analytical rotating field equations. In the first step, the permeance of the stator is calculated for one slot pitch, which is shown in Fig. 2. This allows us to describe the magnetic circuit and the influence of slotting in the simulation. In a second step, the field excitations in the stator and rotor are implemented. The field of the permanent magnets in the rotor is approximated through a sinusoidal field wave of the rotor, neglecting any geometrical design in the rotor topology. The

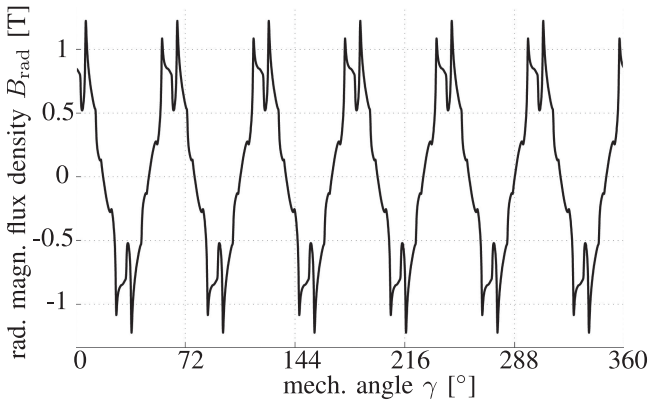

Fig. 3. Radial air gap flux density B_{rad} for analytical approach with CM. Regarding number of pole pairs $p = 6$, the spatial order 6 is dominant.

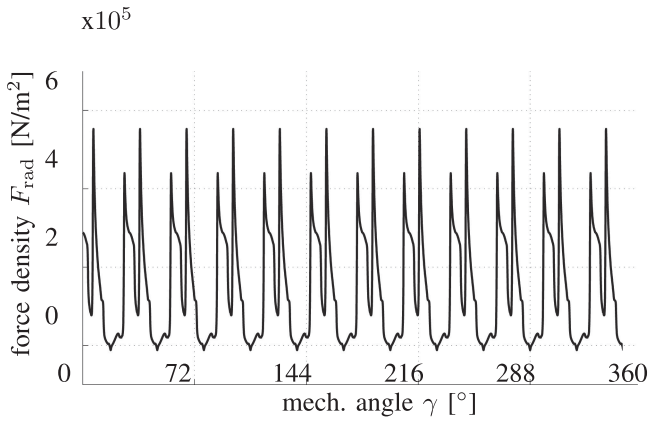

Fig. 4. Radial force density F_{rad} at stator teeth for approach with CM. Regarding the description of one time step, force density orders 12 and 36 are dominant.

field excitation in the winding of the stator is also described by a sinusoidal excitation function, neglecting any current ripple produced by the converter. The resulting air gap flux density is shown in Fig. 3. In the third step, the force density is calculated depending on the air gap flux density, which is shown in Fig. 4. This approach is considered for a force density calculation in the air gap of the machine and adaptable to a structure dynamic model regarding the deformation of the drive train.

3) Numerical Model Based on FEA: The third considered approach for electrical machine modeling is a numerical model based on FEA. Therefore, a 2-D model of the cross-sectional geometry of the machine is constructed, with regard to a detailed adaption to the original machine. The design of the rotor topology with flux barriers and corresponding bridge design, the shape of the tips of the stator teeth, and other relevant parameters are included. For comparison of the numerical model and the analytical model, based on CM, the torque distribution for the nominal operating point with peak phase current $I_{\mathrm{ph}} = 300$ A and control angle $\psi_{\mathrm{opt}} = 10°$ is shown in Fig. 5. The evaluation data in Table II show that the mean value of resulting torque is similar in both approaches, and referring to that, the approach based on CM is more beneficial, according to shorter calculation

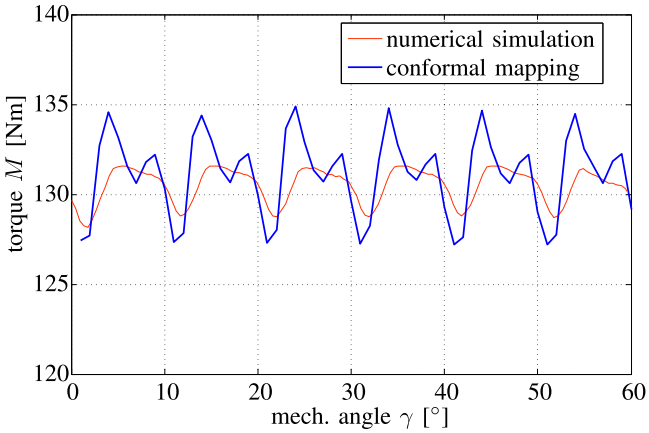

Fig. 5. Torque distribution regarding one pole pair (60°). Simulation with the analytical model based on CM (blue line) and with the numerical model in FEA (red line). The calculation is performed for nominal peak phase current $I_{\mathrm{ph}} = 300$ A and control angle $\psi_{\mathrm{opt}} = 10°$. Nominal torque M regarding maximum torque per ampere (MTPA).

TABLE II
COMPARISON OF TORQUE DISTRIBUTION

Parameter	CM	FEA	Difference in %
mean torque [N·m]	131.1	130.5	0.5
torque ripple [N·m]	7.7	3.5	54.5
calculation time [min]	2.0	20.0	90.0

time for one operating point of the machine. For the evaluation of acoustic phenomena, the numerical approach is more detailed concerning the modeling of the magnetic circuit, which shows the difference in the torque ripple in Table II. For this reason, the numerical approach is considered for further evaluation of force density modeling.

B. Force Calculation

The force excitation model is based on the 2-D FEA simulation presented in Section III-A3. The radial force density at the surface of the stator teeth is locally calculated for every node of the FEA mesh using the eggshell approach [10] (see Fig. 6). Additionally, the torque distribution, resulting of the tangential force density of the machine, is evaluated. The radial force density wave is transformed from the time into the frequency domain via 2-D fast Fourier transformation and sorted in a grid (see Fig. 7). The calculation is performed for every operating point of the IPMSM, described in the dq plane with sinusoidal peak phase current I_{ph} and control angle ψ (see Fig. 8). The grid is used as interface to a 3-D structure dynamic model of the drive train. The coupling of the 2-D and the 3-D model components is performed by the multislice method [11], [12] (see Fig. 9).

1) Local Force Density Distribution: For the local force density distribution, a node-based calculation for every node on the surface of the stator of the machine is performed (see Fig. 6). The resulting force density is described as time and spatial dependent wave. For the evaluation, a 2-D matrix is established,

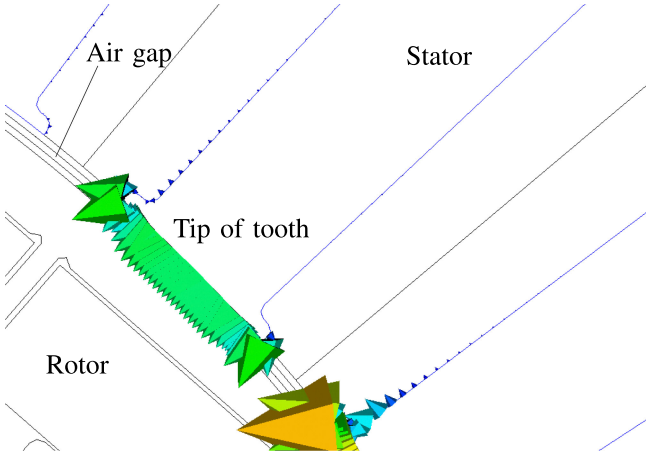

Fig. 6. Force density distribution on stator teeth of electrical machine. Node-based calculation for every node on the surface of the stator (spatial dependence). Calculation for $k = 120$ simulation steps with step width $\theta_{\mathrm{step}} = 0.5°$ (60° part model of the machine for reasons of symmetry).

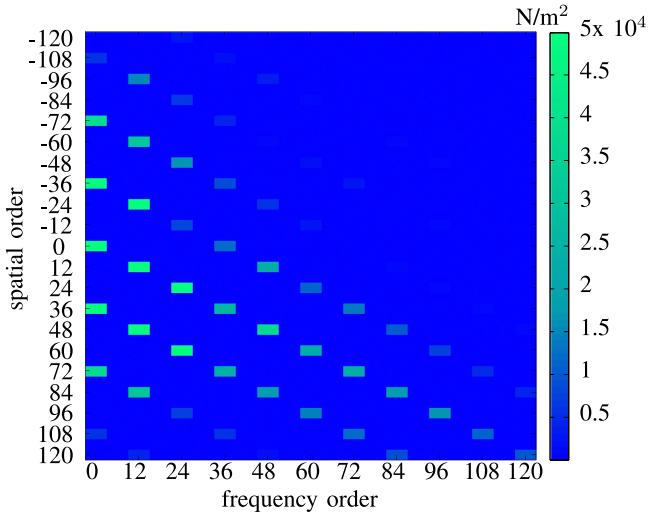

Fig. 7. Evaluation grid for amplitudes of force density distribution in the frequency domain. Absolute values of complex force density coefficients. Evaluation on stator teeth of the machine. Nominal operating point with peak phase current $I_{\mathrm{ph}} = 300\,\mathrm{A}$ and control angle $\psi_{\mathrm{opt}} = 10°$. Constellation with spatial order 0 and frequency order 36 dominant for acoustic emission (first slot harmonic at order 36).

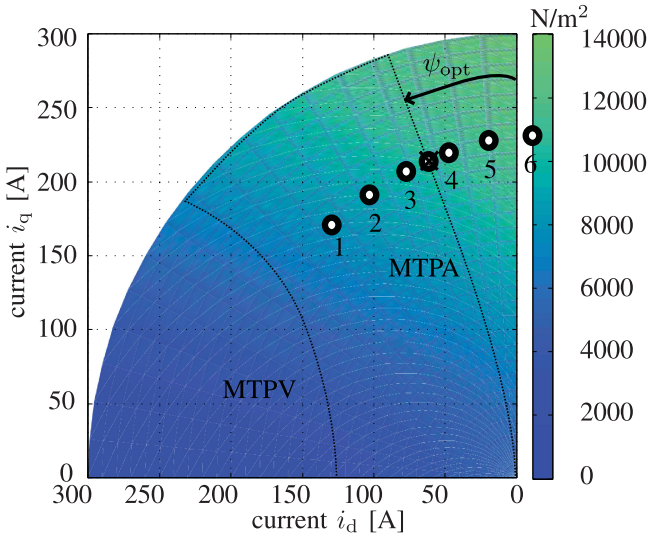

Fig. 8. Electromagnetic operating points in the dq plane. Force density coefficient for frequency order 36 and spatial order 0. Simulation of peak phase currents I_{ph} between 0 and 300 A in 10-A steps (31 values). Simulation of control angles ψ between $-30°$ and 120° in 5° steps (31 values). Different operating points (1–6) for adaptation to slices of the multislice method (see Fig. 9). Control area for maximum torque per ampere (MTPA) and maximum torque per volt (MTPV).

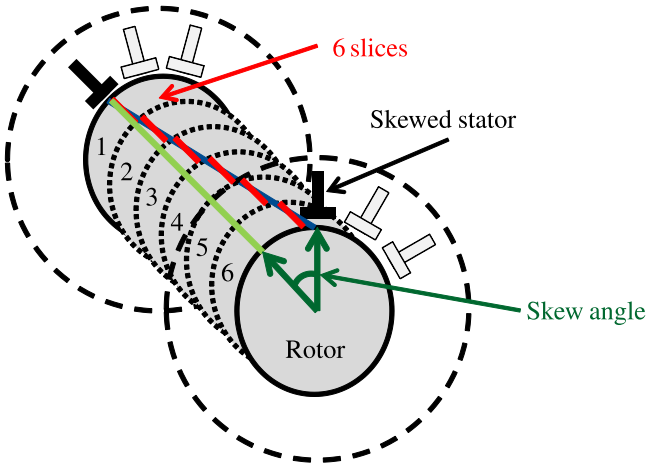

Fig. 9. Simulation with the 2-D model considering skewing of the stator. The multislice method [11], [12] with six slices in axial direction. Adaption in the structure dynamic model by shifting the mechanical position and the operating point of each slice.

containing complex force density vectors. The size of the force density vectors shows that the force density input at the tip of the stator teeth is dominant relating to the slots. For this reason, any deforming effects in the slots are neglected in the structure dynamic model.

2) Interface to Structure Dynamic Model: The interface between force excitation model and structure dynamic model is realized by lookup tables for the torque distribution and the radial force densities. The complex Fourier amplitudes in the frequency domain are transferred in a matrix. Therefore, the torque is transmitted in frequency orders and the radial force density in frequency and spatial orders, resulting of the grid diagram in Fig. 7. In this figure, the relevant frequency orders are shown on the horizontal axis and the spatial orders on the vertical axis. The electrical machine has 12 poles, and therefore, relevant orders are multiples of 12 (compare Fig. 4). The evaluation of force densities, deformations, surface velocities, and, finally, the sound pressure and noise indicate that many order constellations of force densities have lower influence on the noise compared to the amplitude depicted in Fig. 7. To identify these relevant orders, some analytical correlations are introduced [8]. The deformation

$$y \propto \frac{F_{\mathrm{rad}}}{(\nu^2 - 1)^2} \tag{1}$$

is proportional to the force density and inversely proportional to nearly the fourth power of the spatial order ν. For this reason, order constellations including the spatial order 0 are dominant compared to higher order constellations. The surface velocity

$$v_s \propto y \cdot f \tag{2}$$

is proportional to the deformation y and the frequency f. For example, for order constellation 0-spatial/36-frequency, the amplitude of the force density in Fig. 7 is about 12.5 kN/m^2. In comparison, for the order constellation 0-spatial/72-frequency, the relevant frequency is twice as much, but the amplitude of the force density is more than 20 times smaller than for the 36th frequency order. For this reason, the surface velocity [see (2)] is more than ten times higher for order constellation 0-spatial/36-frequency in comparison to order constellation 0-spatial/72-frequency. Frequency order 0 has no influence on the surface velocity. Combining the evaluations for spatial and frequency orders, the constellation 0-spatial/36-frequency of force densities has the most dominant influence on the acoustic behavior of the electrical machine. Since the machine has 36 stator slots, this is the first slot harmonic.

The electromagnetic simulation is performed for various operating points in the operating area, which is shown in Fig. 8. For the control angle ψ, a 30° expansion of the operating area is intended to consider the skewing of the stator with the multislice method [11], [12] (see Fig. 9). With this approach, the machine is axially divided into six slices, and each slice is handled as 2-D cross-sectional element without skewing. With the 2-D simulation of the machine, the resulting torque and radial force density can be adapted to each slice. Concerning the skewing of the stator in axial direction, the simulation results for torque and radial force density have to be mechanically shifted. Additionally, the mechanical shift produces a mismatch of the simulation results relating to the operating point of the machine in a specific slice. Therefore, the corresponding operating point has to be identified in the dq diagram, and the results of torque and radial force density will be connected to the chosen slice.

IV. Validation of Model Chain

To validate the model chain, different test bench scenarios were designed. In the first step, the electrical machine is analyzed on a test bench separately to identify electrical-machine-dependent influences. Measurement results of the surface acceleration on the machine are presented in Fig. 10. To evaluate the measurement results, a spectral analysis for a run-up of the machine is shown. Besides the diagram, the order levels of all orders in summation and the dominant orders 36 and 72 of the first and second slot harmonic are depicted. Fig. 10 shows that especially for resonances at 2600 and 3100 r/min, the slot harmonics describe the main influence for the vibration behavior. The corresponding drive train test bench for the validation of the structure dynamic model is presented in Fig. 11. The approach for this model is presented in Section V. In a last validation step, the electric vehicle is measured on a test track to identify the acoustic behavior at the driver's position. The approach for the acoustic model and simulation results are presented in Section VI.

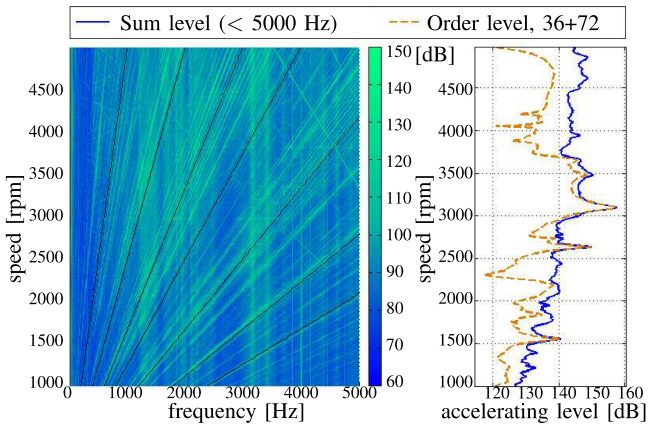

Fig. 10. Measurement of surface acceleration on electrical machine. Spectral analysis between 0 and 5000 Hz. Identification of dominant slot harmonics in order 36 and 72.

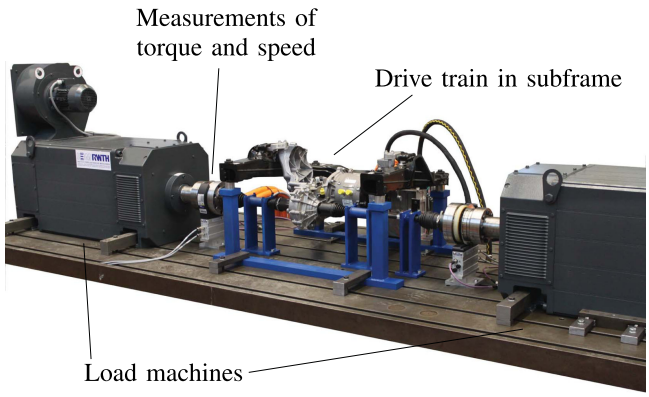

Fig. 11. Test bench for drive train measurements. Entire subframe with electrical machine, gear, differential, side shaft, and wheel bearing. Measurement for different operating points of the electrical machine. Besides general machine measuring data such as torque, speed, current, voltage, temperature, etc., the focus is on the surface acceleration.

V. Structure Dynamic Model

The structure dynamic model of the considered drive train includes, besides the electrical machine, a gearbox, differential, side shaft, and supporting elements to place the electric drive train into the subframe of the electric vehicle. The corresponding model is shown in Fig. 12. In this model, the structure dynamic behavior of the drive train is calculated. A modal analysis of the structure dynamic behavior is performed. It depends on the radial force density, which is applied on the tip of the stator teeth, according to the multislice method presented in Section III-B2. Additionally, the effective torque and the appropriate harmonics are applied on the rotor to adapt the influence of rotational vibrations. The resulting surface velocity of the drive train is used as input parameter for the acoustical model, transforming simulated forces and velocities into binaural sound pressure signals. For the validation of the model, specific measurement

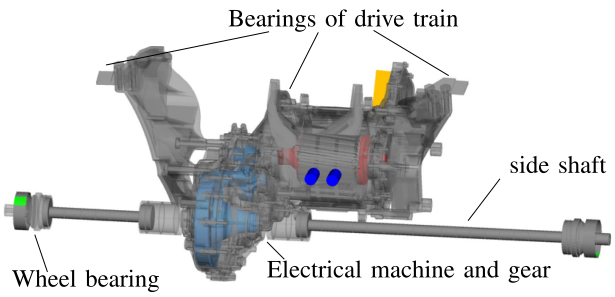

Fig. 12. Structure dynamic model of the drive train, including electrical machine, gear, differential, side shaft, wheel bearings, and supporting arms, to adapt the drive train in the chassis. Dynamic simulation of the structure behavior is performed, depending on the force excitation entry, which is presented in Section III.

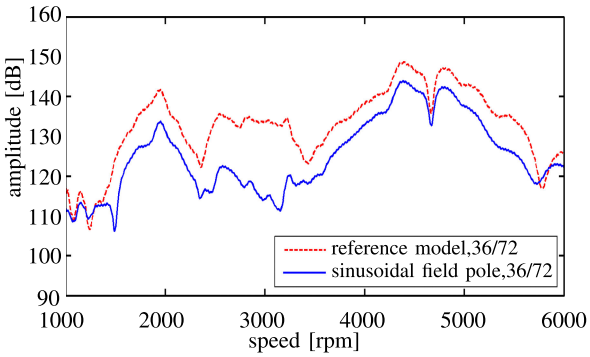

Fig. 13. Order level for the surface acceleration. Simulation point at the side bearing, connecting the drive train with the chassis of the vehicle. Dominant orders 36 and 72 filtered. Resonance of the machine measurements (see Fig. 10) at 3100 r/min is not identified at this position. Simulation for reference model (red line), which is placed in the original electric vehicle and for sinusoidal field pole model (blue line), which is a variation to improve acoustic behavior by designing the rotor of the electrical machine.

points are defined, which are measured on the drive train test bench (see Section IV) and also identified in the simulation model. In Fig. 13, the order level for the surface acceleration is simulated. The orders 36 and 72 are selected, because of their dominant influence as first and second slot harmonic to the force excitation. The simulation is performed at the position of a side bearing of the drive train, which is adapted with an elastomer support to the chassis of the vehicle. To identify any influence of the machine modeling, the simulation was performed for the original electrical machine which is described as reference model, and also for a modified machine design.

The rotor of the modified machine is designed with sinusoidal field poles [13]. The modification is performed by variation of the iron shape at the surface of each rotor pole. The width of the air gap changes, depending on the position angle, between 0.7 (pole center) and 2.1 mm (between two poles). Under consideration of a more sinusoidal air gap flux density distribution, less harmonics in the force densities are excited and lower noise is achieved.

In Table III, the Fourier transformed amplitude of radial force density is evaluated for both the reference model and the modified sinusoidal field pole model for selected constellations of

TABLE III
COMPARISON OF FOURIER TRANSFORMED AMPLITUDES OF FORCE DENSITY ON THE SURFACE OF THE STATOR TEETH

Spatial order	Frequency order	Reference model [N/m^2]	Modified model [N/m^2]
0	36	12 490	4420
12	12	233 900	229 900
24	24	61 760	69 930

spatial and frequency orders. The table shows that some order constellations have an increase in force density, while others decrease. Therefore, it is important to evaluate the surface velocity, described in (1) and (2), because the higher spatial order harmonics with large force density have a negligible influence on the produced noise. For example, the constellation 24-spatial/24-frequency is 12% larger in the modified machine design with sinusoidal field pole than in the reference model. But the deformation is more than 300 000 times smaller than for constellation 0-spatial/36-frequency [see (1)]. To summarize the modification results, the sinusoidal field pole is a beneficial procedure to improve the acoustic behavior of electrical machines. The reduction of the first slot harmonic, mainly presented by order constellation 0-spatial/36-frequency, results in 35% of the force density in comparison to the reference model. Some order constellations are increased by the modification, but their influence is negligible.

Fig. 13 shows the decrease of surface acceleration between the two machine models, depending on the machines speed and, therefore, excitation frequency.

VI. ACOUSTIC MODEL

For the acoustic model, an auralization and psychoacoustical evaluation is performed to describe the noise at the driver's position [14]. The drive train components are approximated as cylindrical and piston-type elements, and the calculated surface velocities of the structure dynamic model are used as input parameter. The vehicle specific transfer paths are determined by measurements on the test vehicle [15]. The structure borne sound is measured from the position of the elastomer supported bearings of the drive train to the driver's ear. The transfer path for airborne sound is measured from the surface of the components to the ear of the driver. To consider the acoustic behavior of a human body, an artificial head with normed earlap and two microphones in both ears is used (see Fig. 1). In the psychoacoustical evaluation, the loudness at the driver's position is evaluated and handled as objective function for the comparison between the original machine design and the machine variation of a sinusoidal field pole topology. The psychoacoustical evaluation is a model-based procedure concerning equal-loudness contours [14]. In future works, a panel test with several people is planned, in order to validate the results.

The total loudness is presented in Fig. 14 for the reference machine design (blue curve) and the modified topology with sinusoidal field pole to improve the waveform of the air gap

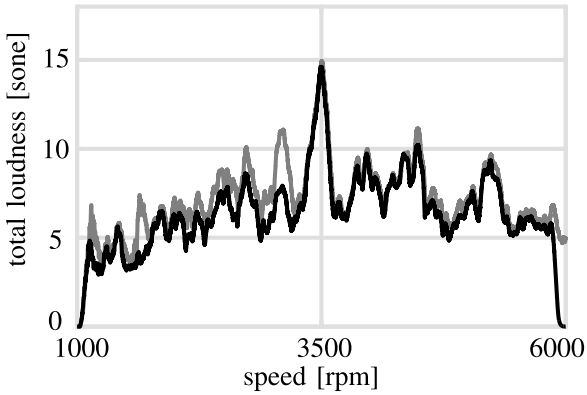

Fig. 14. Psychoacoustic simulation of total loudness at the driver's position. Integration over the entire frequency spectrum while driving the electrical machine to 6000 r/min (speed of electric vehicle: 60 km/h). Loudness is specified with psychoacoustic unit sone, which describes how loud the noise is perceived by the human ear. Comparison of reference machine in original vehicle (gray curve) and machine with modified rotor as sinusoidal field pole (black curve).

flux density (red curve). In Fig. 14, the resonances for different speed levels are shown. The loudness is integrated along the entire considered frequency area between 0 and 5000 Hz. The loudness is observed for the operating area between 1000 and 6000 r/min, which was identified in the test track with conspicuous noise. The results in Fig. 14 show a decrease with the machine variation for the loudness in the entire considered operating area. Especially, for lower speed, an improvement of the sound behavior is displayed. At the speed of 3100 r/min, a resonance is totally reduced for the improved topology. This resonance results of the force density excitation order 36 of the machine, which is shown in the measurement results in Fig. 10.

VII. Conclusion

In this paper, a model chain to describe the acoustic behavior of an electric vehicle was introduced. The complete model chain, starting with the operating point of the electrical machine and resulting in the psychoacoustical evaluation of the loudness at the driver's position, has been considered. Each model component was validated with test bench measurements. The work focuses on the electrical machine design, force excitation process, and interface to the structure dynamic model. The modular design concept allows the replacement of different parts of the model. For example, if the machine in the specific vehicle is replaced, only the force excitation model has to be updated due to the new machine concept. The presented method is adaptable to different concepts of electrical machines and drive trains. It is applicable to various applications that have an electrical drive train and is focused on noise reduction. The results of the total model chain were used to find beneficial topologies for the rotor geometry of the machine. The topologies were adjusted to ensure a more sinusoidal waveform of air gap flux density and, therefore, an improvement in harmonics of force density and torque. The model chain gives the possibility of reaching a beneficial acoustical design of the drive train components with focus on the electrical machine.

References

[1] T. Küppers, "Results of a structured development process of electric vehicle target sounds," presented at the Aachen Acoust. Colloq., Aachen, Germany, 2012.
[2] G. Eisele, "Electric vehicle sound design—Just wishful thinking," presented at the Aachen Acoust. Colloq., Aachen, Germany, Nov. 22–24, 2010.
[3] S. Rick, A. K. Putri, D. Franck, and K. Hameyer, "Hybrid acoustic model of electric vehicles: Force excitation in permanent magnet synchronous machines," in *Proc. IEEE Int. Electr. Mach. Drives Conf.*, 2015, pp. 1419–1425.
[4] K. Genuit and W. R. Bray, "Prediction of sound and vibration in a virtual automobile," *Sound Vib.*, pp. 1–7, Jul. 2002.
[5] M. Wegerhoff and G. Jacobs, "Hybrid NVH simulation for electrical vehicles II—Structural model," in *Proc. Annu. Conf. Acoust. Prog. Acoust.*, Nuremberg, Germany, 2015, pp. 1289–1291.
[6] J. Klein, G. Behler, and M. Vorländer, "Hybrid NVH simulation for electrical vehicles III—Acoustic model," presented at the Annu. Conf. Acoust. Prog. Acoust., Nuremberg, Germany, 2015.
[7] J.-B. Dupont and P. Bouvet, "Noise radiated by an electrical powertrain: Multiphysical simulation," presented at the 21eme Congres Francais de Mecanique, Bordeaux, France, 2013.
[8] H. Jordan, *Geräuscharme Elektromotoren, Lärmbildung und Lärmbeseitung bei Elektromotoren*. Essen, Germany: W. Girardet, 1950.
[9] M. Hafner, D. Franck, and K. Hameyer, "Static electromagnetic field computation by conformal mapping in permanent magnet synchronous machines," *IEEE Trans. Magn.*, vol. 46, no. 8, pp. 3105–3108, Aug. 2010.
[10] F. Henrotte and K. Hameyer, "A theory for electromagnetic force formulas in continuous media," *IEEE Trans. Magn.*, vol. 43, no. 2, pp. 1445–1448, Apr. 2007.
[11] F. Piriou and A. Razek, "A model for coupled magnetic-electric circuits in electric machines with skewed slots," *IEEE Trans. Magn.*, vol. 26, no. 2, pp. 1096–1100, Mar. 1990.
[12] C. Schlensok, D. van Riesen, D. Seibert, and K. Hameyer, "Fast structure-dynamic simulation of electrical machines using 2D-3D-coupling," in *Proc. 6th Int. Conf. Comput. Electromagn.*, 2006, pp. 1–2.
[13] A. K. Putri, S. Rick, D. Franck, and K. Hameyer, "Application of sinusoidal field pole in a permanent magnet synchronous machine to improve the acoustic behavior considering the MTPA and MTPV operation area," in *Proc. IEEE Int. Electr. Mach. Drives Conf.*, 2015, pp. 1359–1365.
[14] H. Fastl and E. Zwicker, *Psychoacoustics*. Berlin, Germany: Springer-Verlag, 1990.
[15] J. Stecher and H. Zeizinger, "Development of a new plastic mount and its influence in vehicle NVH," presented at the Aachen Acoust. Colloq., Aachen, Germany, 2013.

Sebastian Rick received the Dipl.-Ing. degree in electrical engineering from RWTH Aachen University, Aachen, Germany, in May 2012.

He has been a Research Associate at the Institute of Electrical Machines, RWTH Aachen University, since June 2012. His research interests include new arts of electrical machines, simulation, and acoustical design of electrical machines.

Aryanti Kusuma Putri received the M.Sc. degree in electrical engineering from RWTH Aachen University, Aachen, Germany, in April 2013.

She has been a Research Associate at the Institute of Electrical Machines, RWTH Aachen University, since June 2013. Her research interests include contactless power transmission, parasitic effects in electrical machines, simulation, and design of electrical machines.

David Franck received the Dipl.-Ing. degree in electrical engineering from RWTH Aachen University, Aachen, Germany, in March 2008.

He then became a Research Associate at the Institute of Electrical Machines, RWTH Aachen University, where he has been a Chief Engineer since 2011. His main research interests include the acoustic behavior of electrical machines.

Kay Hameyer (M'96–SM'99) received the M.Sc. degree in electrical engineering from the University of Hanover, Hanover, Germany, in 1986, and the Ph.D. degree from the University of Technology Berlin, Berlin, Germany, in 1992, for work on permanent-magnet excited machines.

After his university studies, he worked with Robert Bosch GmbH, Stuttgart, Germany, as a Design Engineer for permanent-magnet servo motors. From 1988 to 1993, he was a Member of the Staff at the University of Technology Berlin. From 1996 to 2004, he was a Full Professor of numerical field computations and electrical machines at the Katholieke Universiteit Leuven, Leuven, Belgium. Since 2004, he has been a Full Professor and the Director of the Institute of Electrical Machines, RWTH Aachen University, Aachen, Germany. His research interest focuses on all aspects of the design, control, and manufacturing of electrical machines and the associated numerical simulation. The characterization and modeling of hard- and soft-magnetic materials is another focus of his work. He has authored/coauthored more than 250 journal publications, more than 500 international conference publications, and four books. His research interests include numerical field computation and optimization, and the design and control of electrical machines, in particular, permanent-magnet excited machines and induction machines.

Dr. Hameyer has been a Member of the German VDE since 2004 and a Fellow of the Institution of Engineering and Technology, U.K., since 2002.